

# Optical spectra of the carbon-oxygen accretion discs in the ultra-compact X-ray binaries 4U 0614+09, 4U 1543-624 and 2S 0918-549

G. Nelemans<sup>1\*</sup>, P.G. Jonker<sup>1</sup>, T.R. Marsh<sup>2</sup> and M. van der Klis<sup>3</sup>

<sup>1</sup>*Institute of Astronomy, University of Cambridge, Madingley Road, Cambridge CB3 0HA, UK*

<sup>2</sup>*Department of Physics, University of Warwick, Coventry CV4 7AL, UK*

<sup>3</sup>*Astronomical Institute “Anton Pannekoek”, University of Amsterdam, Kruislaan 403, NL-1098 SJ Amsterdam, the Netherlands*

Accepted . Received 30 October 2018

## ABSTRACT

We present optical spectra in the range 4600 – 8600 Å for three low-mass X-ray binaries which have been suggested to belong to the class of ultra-compact X-ray binaries based on their X-ray spectra. Our spectra show no evidence for hydrogen or helium emission lines, as are seen in classical X-ray binaries. The spectrum of 4U 0614+09 does show emission lines which we identify with carbon and oxygen lines of C II, C III, O II and O III. While the spectra of 4U 1543-624 and 2S 0918-549 have a lower signal-to-noise ratio, and thus are more difficult to interpret, some of the characteristic features of 4U 0614+09 are present in these spectra too, although sometimes they are clearly weaker. We conclude that the optical spectra give further evidence for the ultra-compact nature of these X-ray binaries and for their donor stars being carbon-oxygen white dwarfs.

**Key words:** binaries: close – stars: individual: 4U 0614+09 – stars: individual: 4U 1543-624 – stars: individual: 2S 0918-549

## 1 INTRODUCTION

Low-mass X-ray binaries are systems in which a neutron star or black hole accretes from a low-mass companion. Most systems have orbital periods of hours to days and are consistent with the scenario (van den Heuvel 1983) in which the donors are main sequence or evolved, hydrogen-rich, stars. A few ultra-compact systems have orbital periods below an hour and are so compact that the donor stars cannot be main sequence stars, but instead must be hydrogen poor (e.g. Verbunt & van den Heuvel 1995).

From X-ray spectra of five X-ray binaries, including the persistent sources 4U 0614+09, 4U 1543-624 and 2S 0918-549 Juett et al. (2001) inferred an enhanced neon/oxygen ratio, which they interpreted as being local to the systems. The similarities between these three systems and the other two, which are known ultra-compact X-ray binaries, led Juett et al. (2001) to conclude that these systems all have ultra-short orbital periods and to propose that their donor stars originally were carbon-oxygen or oxygen-neon-magnesium white dwarfs. Recently, Juett & Chakrabarty (2003) reported further X-ray spectroscopy for 4U 1543-624 and 2S 0918-549, confirming their earlier findings. Yungelson, Nelemans & van den Heuvel (2002) ar-

gued, based on mass-transfer stability arguments, that the donor stars in ultra-compact X-ray binaries that have formed from white dwarf – neutron star binaries should be low-mass white dwarfs ( $M_{\text{donor}} \lesssim 0.45M_{\odot}$ ). Combining binary evolution constraints and white dwarf interior studies, Yungelson et al. (2002) concluded that these systems could be brought into one unifying scheme in which the systems were descendants of binaries consisting of a so called hybrid white dwarf (carbon-oxygen (CO) core with thick helium mantle, Iben & Tutukov 1985) and a neutron star. The systems came into contact by angular momentum loss due to gravitational wave emission, and quickly evolved from periods of a few minutes to typical periods of tens of minutes. After cooling for several Gyr the interior of a CO white dwarf crystallises and, due to differential gravitational settling, chemical fractionation will occur (e.g. Hernanz et al. 1994). At periods above 10 minutes neon enriched layers could be exposed (see Yungelson et al. 2002). At these orbital periods the only alternative donor stars are degenerate helium stars or hydrogen poor remnants of stars that started mass transfer at the very end of the main sequence (for the latter, see Podosiadlowski et al. 2003), which would consist mainly of helium.

To further test the possible ultra-compact nature of 4U 0614+09, 2S 0918-549 and 4U 1543-624, we obtained optical spectra for these sources, because ultra-compact systems are expected to be hydrogen deficient, and even more, neon-rich donors stars are also expected to be helium deficient. Previous optical spec-

\* E-mail: nelemans@ast.cam.ac.uk, based on observations made with ESO Telescopes at the Paranal Observatories under programme ID 071.D-0119

**Table 1.** Log of the observations

date, UT	grism	exp.time (s)	airmass	seeing
<b>4U 0614+09</b>				
23/04/2003, 23:41:13	1400V	2341	1.66	0.9
24/04/2004, 23:30:29	600RI	2341	1.61	~1.3
<b>4U 1543-624</b>				
25/04/2003, 09:10:06	1400V	2661	1.47	~0.5
27/04/2003, 06:17:24	1400V	2301	1.26	1.3
25/04/2003, 08:17:31	600RI	2661	1.36	~0.5
<b>2S 0918-549</b>				
27/04.2003, 23:57:33	1400V	2661	1.16	0.5
30/04/2003, 01:31:59	1400V	2301	1.26	1.3
30/04/2003, 00:40:22	600RI	2661	1.19	0.7

tra of 4U 0614+09 (Davidsen et al. 1974; Machin et al. 1990) indeed show no signs of the classical accretion disc hydrogen emission lines but have a relatively low S/N ratio.

## 2 OBSERVATIONS AND REDUCTION

Spectra were taken with the FORS2 spectrograph on UT4 of the 8m Very Large Telescope on Paranal in Chile. For each object we took spectra both with the 1400V and 600RI holographic grisms, with a 1" slit, using 2x2 on-chip binning. This setup resulted in coverage of 4620 – 5930 Å with mean dispersion of 0.64 Å/pix for the 1400V spectra and 5290 – 8620 Å with mean dispersion of 1.63 Å/pix for the 600RI spectra. A log of the observations is given in Table 1.

Data reduction was done using standard IRAF<sup>1</sup> tasks. The bias was removed using the overscan region of the CCD, after which the images were flatfield corrected using the standard calibration plan flatfields. Spectra were extracted using optimal extraction (Horne 1986) with the `apa11` task. Arc lamp spectra were extracted from the same place on the CCD. The 1400V wavelength calibration was obtained using the positions of 17 lines, giving a root-mean-square scatter of 0.05 Å in fitting a fourth-order Lagrangian polynomial. The 600RI wavelength calibration uses 40 lines and gives a root-mean-square scatter of 0.15 Å for a fourth-order Lagrangian polynomial.

The spectra were flux calibrated, using the nearest two flux standard stars that were available from the VLT archive. Since these were taken many days from our observations the flux calibration only provides a very rough absolute flux calibration, but it does give a reasonable estimate of the continuum shape. The reduced spectra were subsequently imported in the MOLLY package for further analysis. For 4U 0614+09, where the S/N ratio is the highest, we removed the telluric absorption features by dividing the flux calibrated spectrum by a template of the absorption. The template was constructed from the spectrum of a bright star that was also in the slit as follows. We fitted a third order cubic spline to line-free regions of the continuum of this spectrum and used the fit to normalise the continuum to unity. The value of all pixels in the spectrum was set to 1, except for the wavelength ranges 6865–7700 and 8085 – 8265 Å, where strong telluric features are present.

For each object all spectra were combined and averaged to obtain one final spectrum.

**Table 2.** Negative equivalent width (–EW) upper limits (3  $\sigma$ ) on H and He lines, spectral shape and reddening determinations

	4U 0614+09	4U 1543-624	2S 0918-549
<b>H and He –EWs (Å)</b>			
H $\beta$ (4861)	< 0.33	–0.53 $\pm$ 0.1?	< 0.36
He I 5876	< 0.22	< 0.33	< 0.36
He I 6678	< 0.41	< 0.58	< 1.0
He I 7065	< 0.40	< 0.49	< 0.73
He I 5015	< 0.26	< 0.29	< 0.35
He I 4713	< 0.24	< 0.21	0.41 $\pm$ 0.09?
He II 5411	< 0.30	< 0.46	< 0.61
<b>Spectral shape</b>			
$\alpha$ ( $F_\lambda \propto \lambda^{-\alpha}$ )	1.67 (1.43)	2.15	1.46
<b>Reddening measurements</b>			
EW Na D lines	1.67 $\pm$ 0.06	2.17 $\pm$ 0.08	1.90 $\pm$ 0.1
$\Rightarrow$ E(B–V)	$\gtrsim$ 0.4	$\gtrsim$ 0.4	$\gtrsim$ 0.4
EW 5780 DIB	0.44 $\pm$ 0.03	0.16 $\pm$ 0.05	0.35 $\pm$ 0.07
$\Rightarrow$ E(B–V)	0.88 $\pm$ 0.1	0.32 $\pm$ 0.1	0.70 $\pm$ 0.15
E(B–V) <sub>max,SFK</sub>	0.51	0.32	0.6
E(B–V) <sub>max,X</sub> <sup>a</sup>	0.64	0.57	0.6

<sup>a</sup> From Juett et al. (2001) using  $N_H = 0.179 A_V 10^{22} \text{cm}^{-2}$  (Predehl & Schmitt 1995) and  $A_V = 3.3 E(B - V)$  (Schlegel et al. 1998).

## 3 ANALYSIS AND INTERPRETATION

### 3.1 Identification of the lines

In Fig. 1 we show the combined spectra. In the figure we also show the positions of the most common hydrogen emission lines seen in classical X-ray binaries as solid vertical lines (H $\alpha$  at 6563 Å and H $\beta$  at 4861 Å). We also show the positions of several helium emission lines observed in optical spectra of some interacting binaries (e.g. GP Com, see Marsh et al. 1991). The dashed lines show He I lines at 4713, 4921, 5015, 5876, 6678, 7065 and 7286 Å. The dotted line shows the position of the He II 4686 Å line often seen together with hydrogen emission. From Fig. 1 it is clear that the objects do not show strong lines of hydrogen or helium. Upper limits on the equivalent widths (EWs) of these lines are shown in Table 2 (where we give the value of –EW to avoid minus signs). There is a hint of absorption around H $\beta$  in 4U 1543-624 and possibly emission around He I 4713 in 2S 0918-54.

The 4U 0614+09 spectrum shows clear, though sometimes weak, emission lines. We propose that these are due to partially ionised carbon and oxygen, which have many lines in the optical region. In order to identify the lines we calculated a simple emission profile for a 30-70 mixture (by number) of carbon and oxygen at a temperature of 27,000 K, using an LTE emission line model, as described in Marsh et al. (1991). We assume a particle density of  $3 \times 10^{13} \text{cm}^{-3}$  and a line of sight through the medium of  $10^7 \text{cm}$ . The only update is that we consider ions up to C V and O V and use an atomic line list compiled from the National Institute of Standards and Technology<sup>2</sup> and the Atomic Line List<sup>3</sup>. The model is smoothed with a 12 Å Gaussian kernel, which at these wavelengths corresponds to a  $\sim 600 \text{km s}^{-1}$  velocity width, if it is associated with kinematics. This model is not a physical model of the accretion disc, as photoionisation is surely important. However, we believe it correctly identifies the lines in the observed spectrum. Almost all features are blends of multiple lines, most of them from C II, C III and O II, while the strong feature at 5585 is due to O III. Around 5810 C IV might be present. In Table 3 we give the posi-

<sup>1</sup> IRAF is distributed by the National Optical Astronomy Observatories

<sup>2</sup> Version 2.0, <http://physics.nist.gov/cgi-bin/AtData/lines.form>

<sup>3</sup> <http://www.pa.uky.edu/~peter/atomic/>

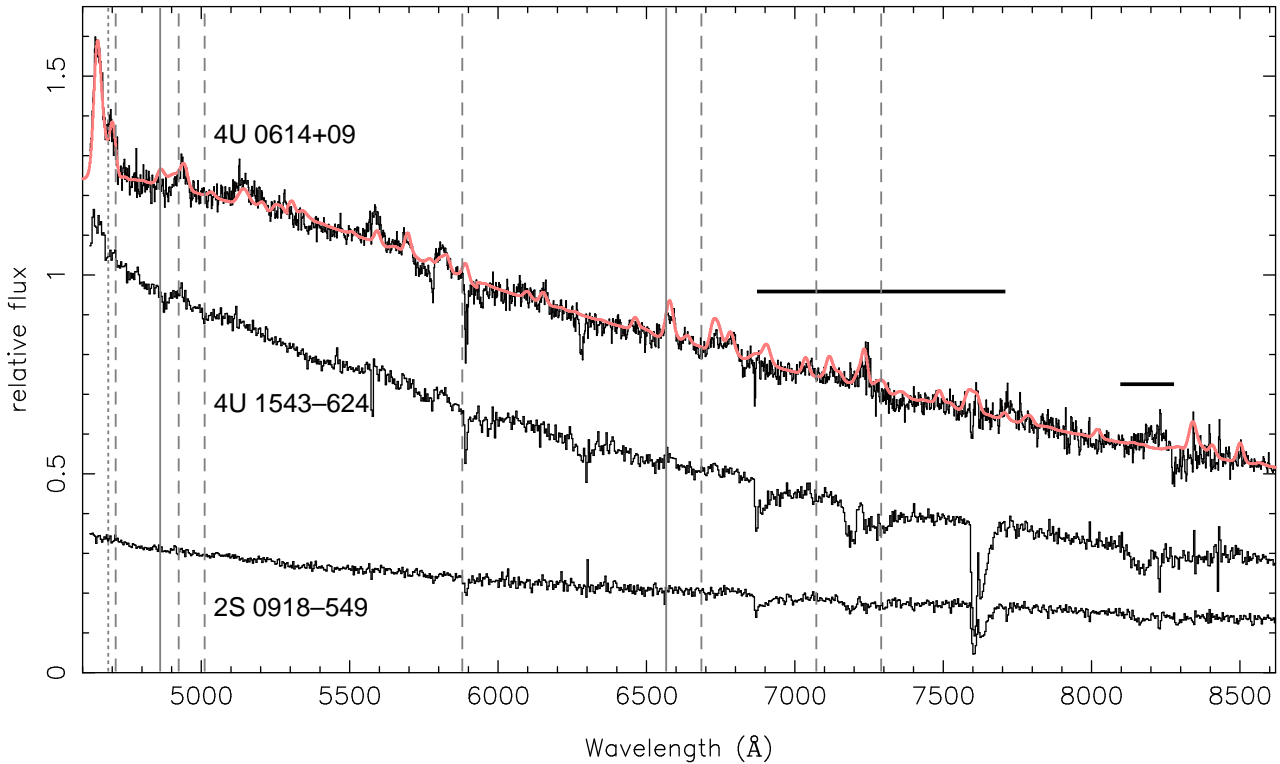


**Figure 1.** Spectra of 4U 0614+09, 4U 1543-624 and 2S 0918-549, rebinned to a scale of 2 or 4 Å/pix. The thick smooth curve plotted over the 4U 0614+09 spectrum shows the pure carbon plus oxygen LTE model used to identify the lines, on top of fit to the continuum. The vertical lines show the wavelength positions of several hydrogen (solid) and helium (dashed, dotted) emission lines seen in hydrogen or helium rich accreting systems. The horizontal bars show the wavelength ranges in which the 4U 0614+09 spectrum is corrected for telluric absorption.

tions of the strongest features and the lines that may contribute to them. We also list the measured equivalent widths of the different features (again negative). The entries within parentheses are either weak lines or uncertain identifications. The 7240 and 8220 features could be affected by the telluric correction.

The lower two spectra in Fig. 1 are of 4U 1543-624 and 2S 0918-549, rebinned to 4 Å to enhance the S/N ratio. In Table 3 we also list the equivalent widths of the features in these spectra. The spectrum of 4U 1543-624 looks like a scaled down version of the 4U 0614+09 spectrum, except maybe for the strength of the C III and O II complexes around 4650 and 4700 Å. All features, except the carbon features at 5280, 6070 and 6150 Å are detected. For 2S 0918-549 the case is less clear, mainly because of the lower signal. The features around 4650, 4700 and 6730 Å are present, but most of the other features are undetected.

### 3.2 Spectral shape and reddening

In Table 2 we also list the measured spectral slope of the three objects, assuming a power law ( $F_\lambda \propto \lambda^{-\alpha}$ ), and the temperatures of the best fitting black body spectra ( $T_{\text{BB}}$ ). The spectrum of 4U 1543-624 is significantly bluer than the other two. For 4U 0614+09, the continuum is well fit with  $\alpha = 1.67$  for  $\lambda \gtrsim 5100$  Å, but is significantly flatter below. This flattening is not seen in the spectrum of Machin et al. (1990), and thus might be due to the flux calibration.

We also list several estimates or limits on the interstellar reddening of the objects. We have two possible reddening indicators available in the spectra: the Na D lines and the diffuse interstellar band (DIB) at 5780 Å. In Table 2 we list the measure equivalent

widths of these features and the implied reddening according to Munari & Zwitter (1997) and Herbig (1993) respectively. The Na D lines only give rough lower limits, as the EWs level off above  $E(B - V) \approx 0.5$  due to saturation. The high EWs measured here would then be the result of multiple components in the lines, as can indeed be seen in the 4U 0614+09 spectrum. In the Table we also list the maximum reddening according to the Schlegel et al. (1998) dust maps and the implied reddening for the hydrogen column found in the spectral modelling of the X-ray spectra (Juett et al. 2001). These last values are upper limits, as the local O and Ne absorption implied by the spectra would artificially enhance the hydrogen column in the fits to the X-ray spectra (e.g. Juett et al. 2001). Although the above gives a barely consistent picture, we conclude that the reddening of these objects is probably close to the maximum in the Galaxy in their directions.

### 3.3 Origin of the line emission

Although detailed modelling of the observed spectra is beyond the scope of this paper, we briefly discuss the possible origin of the line emission. The spectral shapes of the continua, corrected for the reddening (using  $E(B - V) = 0.6, 0.4$  and  $0.6$  for 4U 0614+09, 4U 1543-624 and 2S 0918-549 respectively) are consistent with a black body of temperature  $\sim 20,000$  K. The fact that these objects are persistent X-ray sources, could point at origin of the lines in either the irradiated disc or the irradiated donor star, although in that case more than doubly ionised species might be expected to be present. Only phase resolved spectroscopy will conclusively tell, but the observed width of the lines ( $\sim 600 \text{ km s}^{-1}$ ) might suggest the inner parts of the accretion disc.

**Table 3.** Strongest features in the 4U 0614+09 spectrum and the (possible) line identifications and measured negative EWs (–EWs, to avoid minus signs) for the three spectra. For each feature the wavelength range over which the EW is determined is given in parenthesis.

Feature	Ion	lines	–EW (Å)			Feature	Ion	lines	–EW (Å)						
			4U 0614+09	4U 1543-624	2S 0918-549				4U 0614+09	4U 1543-624	2S 0918-549				
4650 (4624- 4680)	C III	4647.418	9.77 ± 0.15	3.34 ± 0.13	1.99 ± 0.15	5585 (5550- 5620)	O III (OV??)	5592.252	3.12 ± 0.12	2.11 ± 0.18	1.38 ± 0.23				
		4650.246													
		4651.016													
		4651.473													
		4652.048													
		4659.058													
		4663.642													
		4665.860													
		4670.49													
		4671.22													
		4671.74													
		4673.953													
		4638.8558	O II	4641.8103						5700 (5675- 5715)	C III	5695.92	1.21 ± 0.095	1.18 ± 0.15	0.44 ± 0.19
		4649.1347													
		4650.8384													
		4661.6324													
		4673.7331													
4676.2350															
4700 (4680- 4720)	O II	4690.888	3.51 ± 0.12	0.80 ± 0.11	1.37 ± 0.13	5810 (5785- 5840)	C III C IV?	5826.42	1.76 ± 0.11	1.29 ± 0.17	0.71 ± 0.25				
		4691.419													
		4698.437													
		4699.011													
		4699.218													
		4701.179													
		4701.712													
		4703.161													
		4705.346													
		4710.009													
4935 (4900- 4960)	O II	4906.830	1.79 ± 0.11	1.04 ± 0.12	0.54 ± 0.13	6070 (6040- 6120)	C II?	6095.29	0.61 ± 0.23	0.77 ± 0.33	–1.52 ± 0.52				
		4924.529													
		4941.072													
		4943.005													
		4955.707													
5140 (5110- 5165)	C II	5132.947	2.40 ± 0.097	1.12 ± 0.10	0.068 ± 0.13	6150 (6130- 6180)	C II (C III)	6151.27	0.56 ± 0.19	0.21 ± 0.25	0.79 ± 0.42				
		5133.282													
		5143.495													
		5145.165													
		5151.085													
		5159.941													
5190 (5160- 5220)	O II	5175.903	1.54 ± 0.099	0.80 ± 0.11	0.38 ± 0.14	6580 (6550- 6600)	C II (O II)	6578.05	3.14 ± 0.15	1.72 ± 0.20	0.55 ± 0.37				
		5190.498													
		5206.651													
5280 (5230- 5310)	C III	5249.112	0.98 ± 0.11	0.36 ± 0.14	–0.15 ± 0.19	6730 (6700- 6760)	C III	6727.48	2.18 ± 0.16	1.91 ± 0.21	1.33 ± 0.38				
		5253.575													
		5272.522													
		5268.301													
		5257.236													
		5259.056													
		5259.664													
		5259.758													
7240 (7210- 7260)	C II	7231.33				6790 (6760- 6820)	C II	6779.94	2.52 ± 0.15	2.42 ± 0.21	3.83 ± 0.38				
		7236.42													
		7237.17													
		7237.17													
		7237.17													
		7237.17													
		7237.17													
		7237.17													
		7237.17													
		7237.17													
7720? (7700- 7750)	C III?	7707.43	1.75 ± 0.23	0.62 ± 0.28	–1.27 ± 0.38	6970 (6940- 6990)	C III	6974.95							
(8220) (8180- 8260)	(O I?)	(8230)	(4.1 ± 0.34)												

#### 4 DISCUSSION

Previous spectra have been interpreted in a different way to that presented here, but were hampered by quite low S/N ratio. For instance Machin et al. (1990), interpreted the strongest lines near 4650 Å and 5590 Å, as the Bowen blend and possibly O I at 5577 Å. They already commented on the intriguing absence of the usual He II 4686 Å line, which casts doubt on the interpretation of the emission at 4650 Å as the Bowen blend, since the Bowen mecha-

nism is driven by helium. The total absence of any sign of helium at any of the positions indicated in the plots strongly argues against (much) helium in the system.

As discussed in the Introduction, Juett et al. (2001) suggested the donor stars originally were carbon-oxygen or oxygen-neon-magnesium white dwarf, while Yungelson et al. (2002) argued they were hybrid white dwarfs. Our spectra thus give further evidence for the interpretation of 4U 0614+09, 2S 0918-549 and 4U 1543-624 as ultra-compact X-ray binaries with carbon-oxygen white

dwarf donors. One very interesting prospect is the determination of the carbon to oxygen ratio in the transferred material from detailed modelling of the disc spectrum, which would give an unprecedented view into the interior of a white dwarf and possibly could be used to constrain the rate of the  $^{12}\text{C}(\alpha, \gamma)^{16}\text{O}$  reaction (see for a discussion and references Straniero et al. 2003).

Further evidence for the ultra-compact nature of 4U 0614+09 and 2S 0918-549 comes from their absolute visual magnitude. Using the magnitudes and reddening of the objects from the low-mass X-ray binary catalogue (Liu et al. 2001) and the distances of these systems of <3 and 4.2 kpc respectively from type I X-ray bursts (Brandt et al. 1992; Cornelisse et al. 2002) we find absolute magnitudes of >5.4 and 6.9 for 4U 0614+09 and 2S 0918-549. These are very faint for X-ray binaries and, from the van Paradijs & McClintock (1994) relation between absolute magnitude, X-ray luminosity and orbital period, suggest periods well below one hour. The derived X-ray luminosities of  $\lesssim 0.01L_{\text{Edd}}$  for 4U 0614+09 (Ford et al. 1996) and  $\sim 0.003L_{\text{Edd}}$  for 2S 0918-549 (Jonker et al. 2001), assuming these are indicative of the average mass accretion rate, give mass transfer rates of  $\sim 3 \times 10^{-10}$  and  $\sim 9 \times 10^{-11} M_{\odot} \text{ yr}^{-1}$  for 4U 0614+09 and 2S 0918-549, assuming accretion of helium in the type I X-ray bursts (see below). Comparing these rates with Fig. 15 of Deloye & Bildsten (2003), suggests orbital periods of 15-20 and 20-30 minutes for 4U 0614+09 and 2S 0918-549.

Finally we note that our findings pose an interesting question concerning type I bursts. As discussed by Juett & Chakrabarty (2003), the bursts observed in 4U 0614+09 (Swank et al. 1978; Brandt et al. 1992) and 2S 0918-549 (Jonker et al. 2001) are all short bursts, which are believed to be caused by hydrogen and/or helium. They suggest that possibly the donor stars still have non-negligible hydrogen fraction, which would have evolved from binaries that start mass transfer close to the end of the main sequence (Nelson et al. 1986; Podsiadlowski et al. 2002). However, these are expected to consist mainly of helium, rather than carbon and oxygen. The alternative Juett & Chakrabarty (2003) suggest, which seems the only remaining option in light of the lack of helium lines in the optical spectrum, is that spallation of the carbon and oxygen nuclei at the impact onto the neutron star (cf. Bildsten et al. 1992) turns them into helium (or possibly hydrogen), which subsequently triggers the burst.

## 5 CONCLUSIONS

We presented optical spectra of the three suspected ultra-compact X-ray binaries 4U 0614+09, 4U 1543-624 and 2S 0918-549. The spectra show no sign of hydrogen or helium emission lines. We identify the observed features as lines of C II, C III, O II and O III. This is in agreement with the interpretation of these sources as ultra-compact X-ray binaries and the expectation that the donor stars in these objects originally were hybrid white dwarfs that have lost most of their mass and now consists mainly of oxygen and carbon. These spectra are thus of accretion discs almost purely made out of oxygen and carbon.

## ACKNOWLEDGMENTS

We thank the referee Janet Drew for comments that improved the paper. We are thankful to Peter van Hoof and the National Institute of Standards and Technology for compiling the atomic line lists

we use. We further thank Lars Bildsten for stimulating discussions. GN acknowledge the hospitality of the Kavli Institute for Theoretical Physics. This work was supported by the National Science Foundation under grant PHY99-07949.

## REFERENCES

- Bildsten L., Salpeter E. E., Wasserman I., 1992, *ApJ*, 384, 143  
 Brandt S., Castro-Tirado A. J., Lund N., Dremin V., Lapshov I., Syunyaev R., 1992, *A&A*, 262, L15  
 Cornelisse R., Verbunt F., in 't Zand J. J. M., Kuulkers E., Heise J., Remillard R. A., Cocchi M., Natalucci L., Bazzano A., Ubertini P., 2002, *A&A*, 392, 885  
 Davidson A., Malina R., Smith H., Spinrad H., Margon B., Mason K., Hawkins F., Sanford P., 1974, *ApJ*, 193, L25  
 Deloye C. J., Bildsten L., 2003, *ApJ*, in press, astro-ph/0308233  
 Ford E., Kaaret P., Tavani M., Harmon B. A., Zhang S. N., Barret D., Grindlay J., Bloser P., Remillard R. A., 1996, *ApJ*, 469, L37  
 Herbig G. H., 1993, *ApJ*, 407, 142  
 Hernanz M., Garcia-Berro E., Isern J., Mochkovitch R., Segretain L., Chabrier G., 1994, *ApJ*, 434, 652  
 Horne K., 1986, *PASP*, 98, 609  
 Iben Jr I., Tutukov A. V., 1985, *ApJS*, 58, 661  
 Jonker P. G., van der Klis M., Homan J., Méndez M., van Paradijs J., Belloni T., Kouveliotou C., Lewin W., Ford E. C., 2001, *ApJ*, 553, 335  
 Juett A. M., Chakrabarty D., 2003, *ApJ*, in press, astro-ph/0206417  
 Juett A. M., Psaltis D., Chakrabarty D., 2001, *ApJ*, 560, L59  
 Liu Q. Z., van Paradijs J., van den Heuvel E. P. J., 2001, *A&A*, 368, 1021  
 Machin G., Callanan P. J., Charles P. A., Thorstensen J., Brownsberger K., Corbet R. H. D., Hamwey R., Harlaftis E. T., Mason K. O., Mukai K., 1990, *MNRAS*, 247, 205  
 Marsh T. R., Horne K., Rosen S., 1991, *ApJ*, 366, 535  
 Munari U., Zwitter T., 1997, *A&A*, 318, 269  
 Nelson L. A., Rappaport S. A., Joss P. C., 1986, *ApJ*, 304, 231  
 Podsiadlowski P., Han Z., Rappaport S., 2003, *MNRAS*, 340, 1214  
 Podsiadlowski P., Rappaport S., Pfahl E. D., 2002, *ApJ*, 565, 1107  
 Predehl P., Schmitt J. H. M. M., 1995, *A&A*, 293, 889  
 Schlegel D. J., Finkbeiner D. P., Davis M., 1998, *ApJ*, 500, 525  
 Straniero O., Domínguez I., Imbriani G., Piersanti L., 2003, *ApJ*, 583, 878  
 Swank J. H., Boldt E. A., Holt S. S., Serlemitsos P. J., Becker R. H., 1978, *MNRAS*, 182, 349  
 van den Heuvel E. P. J., 1983, in Lewin W. H. G., van den Heuvel E. P. J. eds., *Accretion-driven stellar X-ray sources*. CUP, Cambridge, pp 303–341  
 van Paradijs J., McClintock J. E., 1994, *A&A*, 290, 133  
 Verbunt F., van den Heuvel E. P. J., 1995, in Lewin W. H. G., van Paradijs J. van den Heuvel E. P. J. eds., *X-ray Binaries*. Cambridge: Cambridge Univ. Press, pp 457–494  
 Yungelson L. R., Nelemans G., van den Heuvel E. P. J., 2002, *A&A*, 388, 546